Distortion of Local Atomic Structures in Amorphous Ge-Sb-Te Phase Change Materials

A. Hirata,[1,2,*] T. Ichitsubo,[3] P. F. Guan,[4] T. Fujita,[1] and M. W. Chen[1,5]
[1]WPI Advanced Institute for Materials Research, Tohoku University, Sendai 980-8577, Japan
[2]Mathematics for Advanced Materials-OIL, AIST-Tohoku University, Sendai 980-8577, Japan
[3]Institute for Materials Research, Tohoku University, Sendai 980-8577, Japan
[4]Beijing Computational Science Research Center, Beijing 100084, People's Republic of China
[5]Department of Materials Science and Engineering, Johns Hopkins University, Baltimore, Maryland 21218, USA

(Received 15 November 2017; revised manuscript received 20 January 2018; published 18 May 2018)

The local atomic structures of amorphous Ge-Sb-Te phase-change materials have yet to be clarified and the rapid crystal-amorphous phase change resulting in distinct optical contrast is not well understood. We report the direct observation of local atomic structures in amorphous $Ge_2Sb_2Te_5$ using "local" reverse Monte Carlo modeling dedicated to an angstrom-beam electron diffraction analysis. The results corroborated the existence of local structures with rocksalt crystal-like topology that were greatly distorted compared to the crystal symmetry. This distortion resulted in the breaking of ideal octahedral atomic environments, thereby forming local disordered structures that basically satisfied the overall amorphous structure factor. The crystal-like distorted octahedral structures could be the main building blocks in the formation of the overall amorphous structure of Ge-Sb-Te.

DOI: 10.1103/PhysRevLett.120.205502

Phase-change recording materials are now widely used for commercial optical media such as rewritable compact, digital versatile, and Blu-Ray discs [1–3]. The recording and erasing functions are driven by ultrafast crystal-amorphous structural changes that occur in tens of nanoseconds, where the reflectivity of the amorphous phase is quite different from that of the crystals [4,5]. A number of experimental and simulation studies have been performed to clarify the rapid structural transition between the crystal and amorphous phases, associated with the optical contrast. An early study using x-ray absorption fine structure (XAFS) analysis [6] indicated that the Ge atoms occupy the tetrahedral sites in the amorphous phase, whereas the same atoms occupy the octahedral-like sites in the crystal with a rocksalt-type [7] configuration. They proposed an umbrella-flip model where the Ge atoms quickly switch positions between two different atomic sites [6,8–10]. This result implies that local atomic structures of the amorphous are totally different from those of the crystal, defying the common sense originally proposed by Zachariasen in 1932 [11]. The importance of two competing crystal structures (rocksalt and spinel type) with similar energies but different local configurations to the change in the electronic properties was subsequently discussed based on electronic state calculations [12]. It was proposed that a spinel-type crystal including both tetrahedral and octahedral local configurations was a good approximation of the amorphous structure. On the basis of these findings, the remarkable structural difference might be an origin of the difference in electronic structures generating the large optical contrast. On the other hand, the opponent results, suggesting the structural resemblance between the amorphous and crystal phases, have been also reported after the proposition of the earlier models. To obtain a plausible three-dimensional structural model, for instance, reverse Monte Carlo (RMC) modeling was performed by fitting the simulated data to experimental x-ray scattering data [13]. This study emphasized the structural similarity between the crystal and amorphous phases, where the amorphous structure can be characterized by even-folded ring structures, analogous to the rocksalt crystal. Further *ab initio* molecular dynamics (MD) simulations revealed that only one-third of the Ge atoms are located on tetrahedral sites, although the remaining Ge and the other atoms are essentially defective octahedral sites (rocksalt crystal-like structure) [14,15]. From a viewpoint of electronic structure, moreover, it has been shown that distortion of octahedral configurations is much more important for changing the bonding nature [16,17], instead of introducing tetrahedra like the umbrella-flip model. Although the significance of octahedra and the remarkable difference in bonding nature have been suggested so far [16–20], direct structural evidence is still lacking. Additionally, it was suggested that the rocksaltlike local configuration plays a crucial role in homogeneous crystal nucleation in this material [21]. Thus, describing the amorphous local structures especially relating to octahedral configurations found in the rocksalt crystal is vital for understanding the distinct difference in the optical properties and the rapid structural changes of these materials.

Though the proposed models must be verified experimentally, the experimental data are usually spatially

 © 2018 American Physical Society

averaged though chemically separated (e.g., using XAFS) and therefore include overlapping information from the different types of local structures. Thus, there is an essential ambiguity in determining the amorphous structure through conventional RMC modeling. For amorphous SiO, for example, we showed that totally different structure models definitely satisfy an identical experimental profile obtained by x-ray scattering [22]. To clarify the local structures without ambiguity, we have been developing local reverse Monte Carlo (local RMC) modeling which can determine the structure in a confined nanoscale space and is particularly dedicated to an angstrom-beam electron diffraction (ABED) technique developed by us [22–24]. Although microscopic structural order has been obtained by high-resolution electron microscope (HREM) imaging [25] and fluctuation electron microscopy (FEM) [26], the combination of local RMC modeling and ABED enables us to obtain local structural details, including determination of the symmetry and distortion mode. In this study, we employed local RMC modeling for ABED data to establish the local structures in as-deposited amorphous $Ge_2Sb_2Te_5$.

Amorphous $Ge_2Sb_2Te_5$ films were fabricated by radio-frequency magnetron sputtering. The experimental details are described in the Supplemental Material [27]. The amorphous nature of the sample was confirmed by the typical mazelike contrast of the HREM images and the halo rings in the diffraction pattern (Fig. S1 [27]). The diffraction pattern, which was the averaged scattering intensity obtained from a wide area (~100 nm), was generally consistent with the reported x-ray scattering data [13]. ABED analyses were also performed for the amorphous $Ge_2Sb_2Te_5$ by scanning the film with a subnanometer probe. When analyzing the ABED patterns, we first calculated the typical diffraction patterns of a rocksalt crystal, which has been reported as a metastable crystalline product in $Ge_2Sb_2Te_5$ [7]. Figure 1(a) shows a schematic of the rocksalt crystal and the three diffraction patterns normal to the [001], [011], and [111] directions with four-, two-, and sixfold symmetry, respectively.

Figures 1(b)–1(d) show three types of characteristic ABED patterns obtained from the amorphous $Ge_2Sb_2Te_5$ film. Note that the ABED patterns shown in Figs. 1(b), 1(c), and 1(d) closely resemble the typical crystalline patterns with four-, two-, and sixfold symmetry [see Fig. 1(a)], respectively. For reference, the peak maxima of the first and second halo rings are indicated by dotted circles in the patterns. All four spots in Fig. 1(b) were found on the first ring, whereas all six spots in Fig. 1(d) were on the second ring. In Fig. 1(c), shorter and longer pairs of spots were found on the first and second rings, respectively. These features clearly indicated that the three typical patterns of the amorphous phase are akin to the [001], [011], and [111] patterns of the rocksalt crystal. In addition, the intensity profiles plotted along the circumferential direction [Fig. 1(e)] verified the four- and sixfold symmetry of the

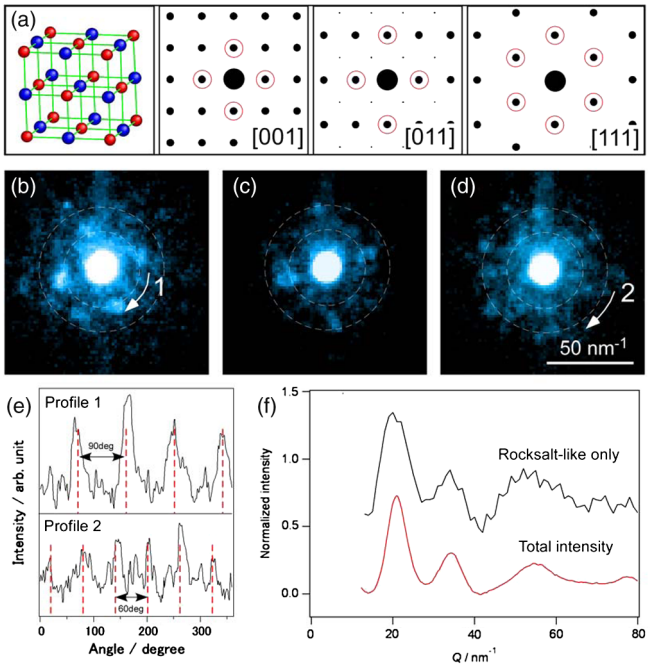

FIG. 1. Experimental ABED patterns from amorphous $Ge_2Sb_2Te_5$ film. (a) Schematic diagram of the rocksalt (NaCl) structure reported for $Ge_2Sb_2Te_5$. Ge and Sb atoms randomly occupy the Na site (blue), whereas Te atoms occupy the Cl site (red). Calculated diffraction patterns of the rocksalt crystal with [001], [011], and [111] incidence directions are also shown. [(b) to (d)] Typical experimental ABED patterns obtained for (b) fourfold rocksalt [001]-type, (c) twofold rocksalt [011]-type, and (d) sixfold rocksalt [111]-type amorphous $Ge_2Sb_2Te_5$. (e) Intensity profiles of fourfold (profile 1) and sixfold (profile 2) patterns along circumferential directions indicated by arrows 1 and 2 in (b) and (d), respectively. For guidance, dotted red lines are shown with distances of 90° and 60° for profile 1 and 2, respectively. (f) Total intensity obtained from normal electron diffraction shown in Fig. S1 [27] (red curve) and accumulated intensity only with rocksaltlike ABED patterns (black curve).

patterns shown in Figs. 1(b) and 1(d). To understand the relationship between these crystal-like patterns and the overall structure, we plotted the intensity profile accumulated from only the three types of patterns (see Fig. S2 [27]) and compared it with the profile of the halo rings (Fig. S1 [27]), as shown in Fig. 1(f). These two profiles were very similar to each other, indicating that the crystal-like local structure was largely distorted to conform to the total halo intensity. In addition, the distorted crystal-like structures were considered the main component of the overall amorphous structure, as only few ABED patterns were required to reproduce the total intensity.

We then used the newly developed local RMC modeling to fit the ABED experimental data without any interatomic potentials [Fig. 2(a)]. Whereas ordinary scattering data contain structural information from bulk samples with a huge amount of atoms (~10^{23} atoms), the present ABED data were generated from only tens of atoms within a local

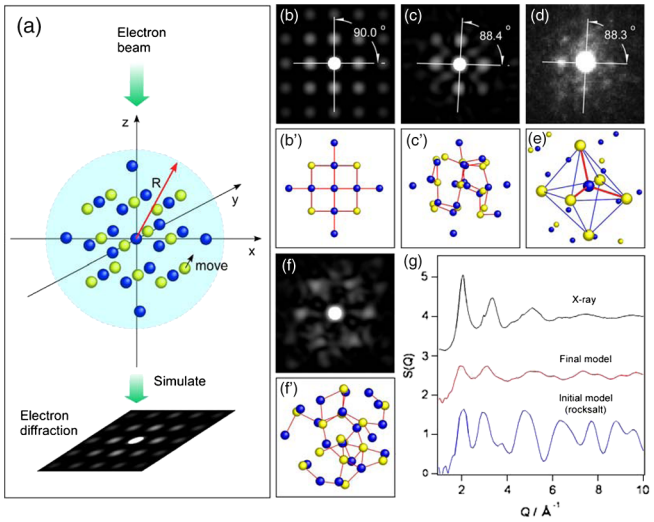

FIG. 2. Local RMC modeling for ABED experiment. (a) Schematic of local RMC modeling. (b) Simulated ABED pattern with fourfold symmetry from the initial rocksalt structure shown in (b'). (c) Simulated ABED pattern from the final model shown in (c'). (d) Experimental ABED pattern used for the modeling. (e) Distorted octahedral configuration in the final model. (f) Simulated ABED pattern with nearly sixfold symmetry from the final model of (f'). The red lines indicate atomic bonds shorter than 0.3 nm, which is equal to the bond length in the rocksalt-type $Ge_2Sb_2Te_5$ crystal. In the models, Ge and Sb atoms randomly occupied the Na site (yellow), whereas Te atoms occupied the Cl site (blue). (g) Structure factor $S(Q)$ profiles calculated from the initial rocksalt and final models shown in (b') and (c'), respectively. For reference, the $S(Q)$ profile obtained from high energy x-ray scattering [13] is also shown.

subnanometer region. Accordingly, the number of atoms fitted to the experimental diffraction data could be significantly reduced using this analysis compared with conventional modeling of standard scattering data (e.g., RMC simulations [28]) and, consequently, uncertainty of the solution could be mathematically minimized. The details of this modeling technique are described in the Supplemental Material (Fig. S7) [27]. To understand the difference between the local structures in the crystal and amorphous phases, the simulation was started from a rocksalt crystal, as shown in Fig. 2(b)'. The corresponding diffraction pattern [Fig. 2(b)] showed a gridlike shape with fourfold symmetry, which is identical to the rocksalt [001] pattern shown in Fig. 1(a). Figure 2(c) shows the simulated diffraction pattern after fitting the [001]-type experimental pattern in Fig. 2(d). It should be noted that the angle between the two diffraction vectors deviated from a right angle (90°) and the diffraction intensity at high scattering angles became much weaker. The structure factor $S(Q)$ of the final model was also close to that of the reported x-ray scattering data, considering the initial rocksalt crystal [Fig. 2(g)]. Note that it was difficult to reproduce the peak height due to the limited number of atoms in the local model. The corresponding structure shown in Fig. 2(c)' was highly distorted compared to the initial structure (Fig. 2(b)'). The structure showed an important feature where only half of the six nearest bonds were significantly shorter than the bonds in the crystal [Fig. 2(e)]. It is also noted that the simulated ABED pattern from the [111]-like orientation [Fig. 2(f)] exhibited nearly sixfold symmetry and reproduces the experimental pattern shown in Fig. 1(d) well.

To confirm local RMC models, an *ab initio* MD simulation was also performed for amorphous $Ge_2Sb_2Te_5$ [Fig. 3(a)]. The calculated $S(Q)$ value agreed well with the previously reported experimental $S(Q)$ [13] (Fig. S3) [27]. We performed Voronoi polyhedral analysis for the obtained MD structure to extract the local crystal-like structures [29]. In the rocksalt crystal structure, each atom has an octahedral environment, so we focused specifically on the octahedra characterized by the Voronoi index of $\langle 0\,6\,0\,0 \rangle$ (Fig. S4) [27] and analyzed their deviation from the crystal structure. The analysis showed that about 12% of the Ge atoms are located in the $\langle 0\,6\,0\,0 \rangle$ octahedral environment and 16% of the Ge atoms have octahedral topology with strong distortion. Note that $\langle 0\,6\,0\,0 \rangle$ octahedra are linked to each other in a continuous manner [Fig. 3(a)]. Figure 3(b) shows the distribution of the length of the bonds between the central atom and the six nearest neighbor atoms for all of the $\langle 0\,6\,0\,0 \rangle$ octahedra in the MD model. Note that all bonds in the rocksalt crystal had a length of 3.0 Å, as indicated by the red dotted line in the figure. For the amorphous phase, a wide range of bond lengths was observed, implying that the octahedra were highly distorted, even though their Voronoi indices were $\langle 0\,6\,0\,0 \rangle$. This fact strongly supports the local RMC model results described in Fig. 2. For the rocksaltlike local atomic arrangements including the $\langle 0\,6\,0\,0 \rangle$ octahedron, we found three orientations similar to the [001], [011], and [111] directions in the crystal by rotating the model [Figs. 3(c)–3(e)]; the ABED patterns were then simulated for each orientation [Fig. 3(c')–3(e')]. It can be seen that the simulated patterns with nearly four-, two-, and sixfold symmetry agreed well with the experimental data shown in Figs. 1(b)–1(d).

In general, conventional RMC modeling for scattering experiments from large-scale specimens provides structural models with a large amount of ambiguity [22]. In contrast, local RMC modeling for ABED data presented here can provide spatially separated information from confined subnanometer regions. Since the number of possible structural models can be greatly reduced through the local RMC modeling, this enables us to discuss some properties based on the more accurate structural information than before.

Even though distinct rocksaltlike diffraction patterns were observed from each local region, the important thing is that the accumulated profile derived from the ABED patterns, which deviate significantly from those of the rocksalt crystal, fit well with the total average intensity measured over a wide area. In addition, the structural factors of the models obtained by local RMC were also

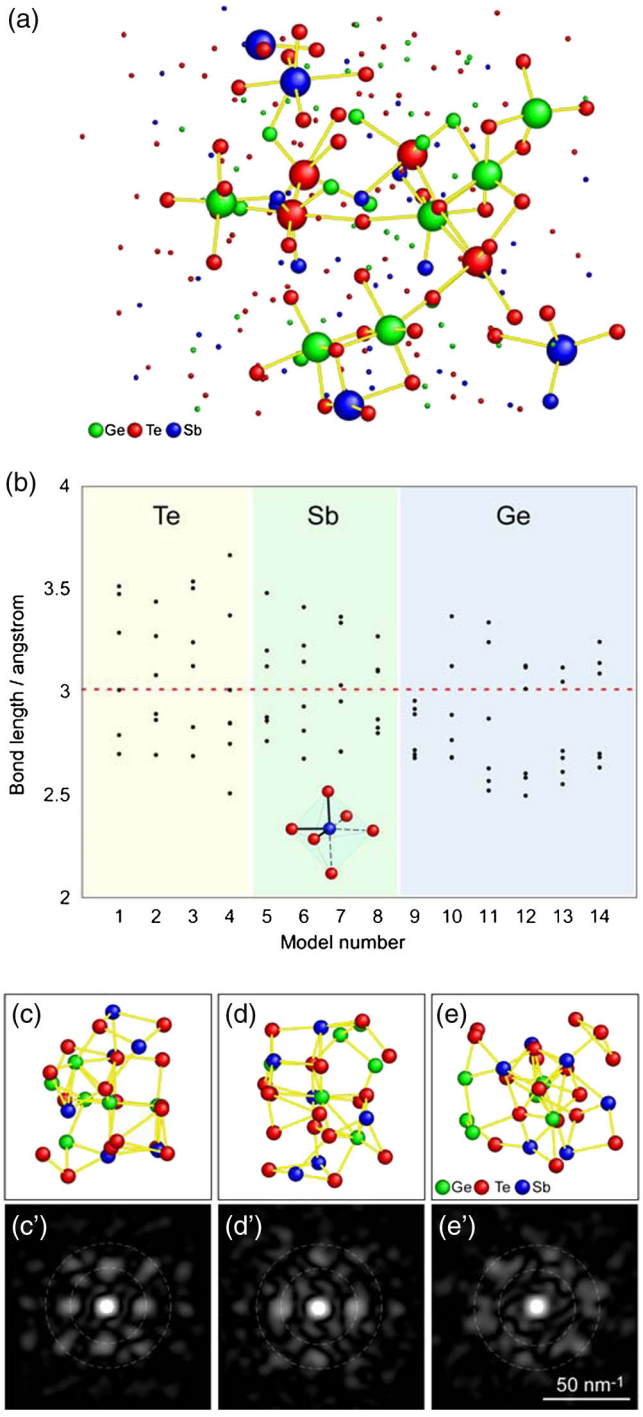

FIG. 3. Rocksaltlike structures in *ab initio* MD model. (a) Schematic of amorphous Ge-Sb-Te model constructed with *ab initio* MD simulation. The large circles denote the central atoms of octahedra indexed by $\langle 0600 \rangle$ in Voronoi polyhedral analysis. Six nearest neighbor atoms are linked to the central atoms with the yellow bonds. (b) Distribution of bond lengths from the central atom to six vertex atoms in $\langle 0600 \rangle$ octahedra. (c) to (e) Rocksaltlike local structures with rocksalt (c) [001]-, (d) [011]-, and (e) [111]-like orientations. The simulated ABED patterns from (c), (d), and (e) are shown in (c'), (d'), and (e'), respectively.

consistent with x-ray scattering results. This implies that the local structures with crystal-like topology were the main building block of the overall amorphous structure, rather than nanocrystals infrequently formed in an amorphous matrix.

Amorphous recording marks in phase change materials are normally formed by the laser annealing [1]. In this study, however, we performed ABED measurement for as-sputtered amorphous $Ge_2Sb_2Te_5$ films prepared using rf magnetron sputtering, not laser-induced amorphous states. Although the sputtered amorphous may be a little less ordered than the laser-induced one formed via crystal melt [25], the rocksaltlike local structures with heavy distortion were clearly observed even in the as-sputtered films. It can be presumed that the rocksaltlike octahedrally configuration is considered as an inherent stable structural unit, which may survive even in the liquid state [21], in this alloy system.

The distortion of the octahedral configurations verified in this study could be smoothly linked with the rattling motion of the central atoms inside octahedra in the initial stage of amorphization as proposed in the previous work [29], and may also be responsible for the change in the electronic structure, e.g., the disruption of resonance bonding in the crystal [16,17,29–31]. Indeed, Huang and Robertson [16] suggested that distortion of octahedra can break up the resonant bonding without introducing any tetrahedra as proposed in the earlier models [6,12]. Our present results would provide direct evidence for the newer mechanism proposed by them [16]. Additionally, the atomic arrangements that are topologically similar to those in the crystal plausibly provide a situation where crystal nucleation occurs with minimal atomic motion [21]. The structures with crystal-like topology observed in this study, which do not necessarily consist of only the first nearest-neighbor atoms [32], are expected to play a role in the rapid rearrangement of the atoms during crystallization.

In summary, ABED analysis was performed on an amorphous $Ge_2Sb_2Te_5$ film to obtain subnanometer scale structural information from local regions. Local atomic structures having the rocksalt crystal-like octahedral configurations were successfully verified by using local RMC modeling for ABED local experimental data. Unlike conventional RMC procedure, the models were determined in a confined nanoscale space based on local ABED data. It was also found that the rocksalt crystal-like local structures mainly contributed to the total intensity obtainable from the wide area. Further, it is highly probable that the octahedrally configurations with the rocksalt crystal-like topology are heavily distorted, breaking the high symmetry of the ideal octahedra expected in the crystal, although the octahedra could be distorted to some extent even in the crystal [33]. In other words, local atomic structures of the amorphous topologically resemble those of the crystal, but they are distinctly different in the sense of a degree of distortion. Considering the model proposed by

Huang and Robertson [16], the symmetry breaking could be closely related to the change in the bonding nature and may, therefore, be responsible for the large optical contrast between the crystal and amorphous phases. This technique is expected to be helpful for delineating the relationship between the optical properties and the degree of local distortion for amorphous phase-change materials.

This work was partially sponsored by Fusion Research Funds from the "World Premier International Research Center Initiative for Atoms, Molecules, and Materials" program of the MEXT of Japan, JSPS KAKENHI (Grants No. JP17H01325 and No. JP26310205), and the Cross-Ministerial Strategic Innovation Promotion Program (Structural Materials for Innovation D72) of the Ministry of Agriculture, Japan. The authors gratefully acknowledge Dr. Shinji Kohara at NIMS for providing us with x-ray scattering data of amorphous Ge-Sb-Te. The authors would like to thank Professor Noboru Yamada at Kyoto University and Professor A. L. Greer at University of Cambridge for the fruitful discussion.

*Corresponding author.
hirata@wpi-aimr.tohoku.ac.jp

[1] M. Wuttig and N. Yamada, Nat. Mater. **6**, 824 (2007).
[2] S. Raoux and M. Wuttig, *Phase Change Materials: Science and Applications* (Springer Science and Business Media, LLC, New York, 2009).
[3] A. V. Kolobov and J. Tominaga, *Chalcogenides: Metastability and Phase Change Phenomena* (Springer-Verlag Berlin Heidelberg, 2012).
[4] S. R. Ovshinsky, Phys. Rev. Lett. **21**, 1450 (1968).
[5] N. Yamada, E. Ohno, N. Akahira, K. Nishiuchi, K. Nagata, and M. Takao, Jpn. J. Appl. Phys., Suppl. **26**, 61 (1987).
[6] A. V. Kolobov, P. Fons, A. I. Frenkel, A. L. Ankudinov, J. Tominaga, and T. Uruga, Nat. Mater. **3**, 703 (2004).
[7] N. Yamada and T. Matsunaga, J. Appl. Phys. **88**, 7020 (2000).
[8] M. Krbal, A. V. Kolobov, P. Fons, J. Tominaga, S. R. Elliott, J. Hegedus, and T. Uruga, Phys. Rev. B **83**, 054203 (2011).
[9] A. V. Kolobov, P. Fons, J. Tominaga, and S. R. Ovshinshy, Phys. Rev. B **87**, 165206 (2013).
[10] M. Micoulaut, A. Piarristeguy, H. Flores-Ruiz, and A. Pradel, Phys. Rev. B **96**, 184204 (2017).
[11] W. H. Zachariasen, J. Am. Chem. Soc. **54**, 3841 (1932).
[12] W. Wełnic, A. Pamungkas, R. Detemple, C. Steimer, S. Blügel, and M. Wuttig, Nat. Mater. **5**, 56 (2006).
[13] S. Kohara *et al.*, Appl. Phys. Lett. **89**, 201910 (2006).
[14] S. Caravati, M. Bernasconi, T. Kuhne, M. Krack, and M. Parrinello, Appl. Phys. Lett. **91**, 171906 (2007).
[15] J. Akola and R. O. Jones, Phys. Rev. B **76**, 235201 (2007).
[16] B. Huang and J. Robertson, Phys. Rev. B **81**, 081204R (2010).
[17] J. Y. Raty, W. Zhang, J. Luckas, C. Chen, R. Mazzarello, C. Bichara, and M. Wuttig, Nat. Commun. **6**, 7467 (2015).
[18] T. Matsunaga *et al.*, Adv. Funct. Mater. **21**, 2232 (2011).
[19] M. Wuttig, V. L. Deringer, X. Gonze, C. Bichara, and J.-Y. Raty, arXiv:1712.03588.
[20] M. Zhu, O. Cojocaru-Mirédin, A. M. Mio, J. Keutgen, M. Küpers, Y. Yu, J.-Y. Cho, R. Dronskowski, and M. Wuttig, Adv. Mater. **30**, 1706735 (2018).
[21] J. Hegedus and S. Elliott, Nat. Mater. **7**, 399 (2008).
[22] A. Hirata, S. Kohara, T. Asada, M. Arao, C. Yogi, H. Imai, Y. W. Tan, T. Fujita, and M. W. Chen, Nat. Commun. **7**, 11591 (2016).
[23] A. Hirata, P. F. Guan, T. Fujita, Y. Hirotsu, A. Inoue, A. R. Yavari, T. Sakurai, and M. W. Chen, Nat. Mater. **10**, 28 (2011).
[24] A. Hirata, L. J. Kang, T. Fujita, B. Klumov, K. Matsue, M. Kotani, A. R. Yavari, and M. W. Chen, Science **341**, 376 (2013).
[25] M. Naito, M. Ishimaru, Y. Hirotsu, and M. Takashima, J. Appl. Phys. **95**, 8130 (2004).
[26] M.-H. Kwon, B.-S. Lee, S. N. Bogle, L. N. Nittala, S. G. Bishop, J. R. Abelson, S. Raoux, B.-k. Cheong, and K.-B. Kim, Appl. Phys. Lett. **90**, 021923 (2007).
[27] See Supplemental Material at http://link.aps.org/supplemental/10.1103/PhysRevLett.120.205502 for the details of ABED analyses and local RMC modeling.
[28] R. L. Mcgreevy and L. Pusztai, Mol. Simul. **1**, 359 (1988).
[29] E. Matsubara *et al.*, Phys. Rev. Lett. **117**, 135501 (2016).
[30] K. Shportko, S. Kremers, M. Woda, D. Lencer, J. Robertson, and M. Wuttig, Nat. Mater. **7**, 653 (2008).
[31] A. V. Kolobov, M. Krbal, P. Fons, J. Tominaga, and T. Uruga, Nat. Chem. **3**, 311 (2011).
[32] K. Ohara *et al.*, Adv. Funct. Mater. **22**, 2251 (2012).
[33] M. Krbal *et al.*, Phys. Rev. B **86**, 045212 (2012).